

# Strength Evaluation of Pin Joints for Crane Structure under Tensile Loads

Tsutomu Hoshii\*<sup>1</sup>  
Takeshige Harada\*<sup>2</sup>

## 1. Introduction

A variety of research has already been done on stress conditions of pin joints for coupling the members of various structures under a tensile load condition. Analysis by the elastic theory<sup>(1)</sup> or by photo elastic experiments<sup>(2)</sup> show that a large stress concentration occurs on the side faces of pin holes perpendicular to the tensile load direction. Also, practical stress calculation methods were used<sup>(3),(4)</sup>. However, for the allowable stress on the structural design only AISC<sup>(5)</sup> specifies it as far as the authors know.

Since many pin joints are used in a crane structure, as shown in Fig. 1, the strength evaluation of these pin joints under a tensile load condition is necessary for giving a safety evaluation. The purpose of this paper is to obtain design information for pin joints by tensile tests and by analysis using the elastic-plastic finite element method.

## 2. Experimental method

### 2.1 Specimens

Fig. 2 shows profiles of specimens. Three kinds of outer radius ratios  $R/r$  1.5 (S type), 2.0 (M type) and 2.5 (L type) are used in this experiment; these ratios are within the range practically used for crane structures.

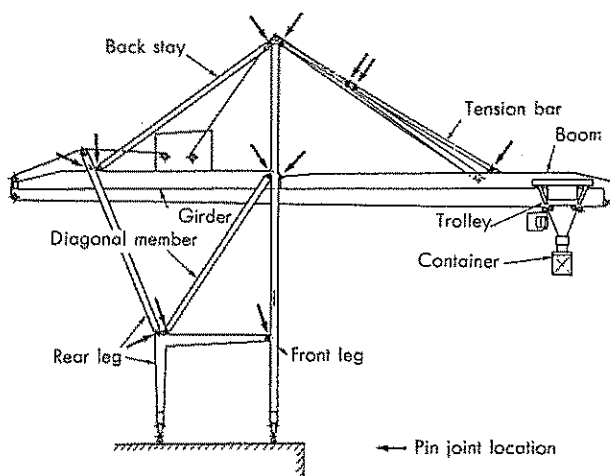


Fig. 1 Pin joints in a container crane

\*<sup>1</sup> Materials Handling Equipment Division, Engineering Department

\*<sup>2</sup> Materials Handling Equipment Division, Quality Assurance Department

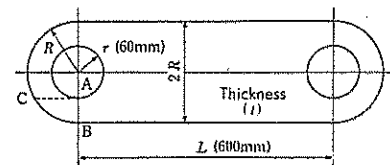


Fig. 2 Specimen profile

Table 1 Mechanical properties of material

Item Material	Tensile strength (MPa)	Yield strength (MPa)	Reduction of area (%)	Elongation (%)
SS41	440	270	68	32

Specimens having three kinds of plate thicknesses ( $t=32, 25, 19$  mm) were employed for the individual outer radius ratio  $R/r$ . These specimens were cut out from SS41 plates and their inner radii were machined so that the clearance from the pins was equivalent to that of the crane structure. Table 1 lists the tensile test results of the specimen materials by JIS 12A specimens.

### 2.2 Experimental device and method

An electric/hydraulic servo 200-ton low cycle fatigue testing machine was employed as a tension tester. Fig. 3 shows its outline. Both ends of a specimen are fixed to the attachments of the testing machine.

A tensile load was gradually applied to the specimen, and the load and the elongation of the specimen were electrically output and recorded. A uniaxial strain gauge

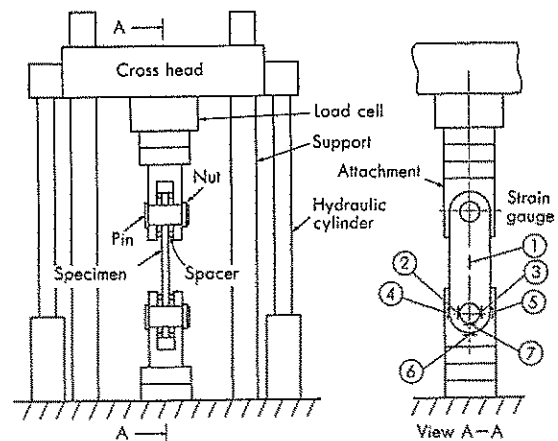


Fig. 3 Outline of experimental device

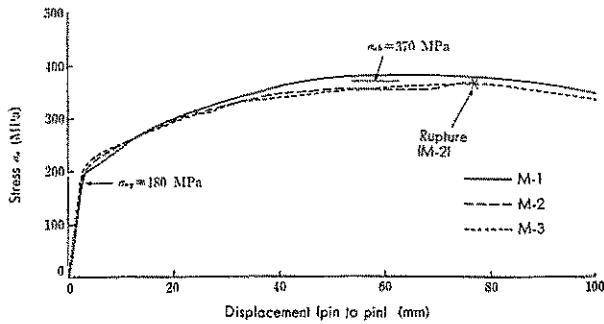


Fig. 4 Relation between tensile stress and displacement (M type)

was bonded to specimens ①—⑦ as shown in Fig. 3 and change of strain at each part due to an increase of tensile load was measured.

### 3. Experimental results

#### 3.1 Yield strength of joints

Fig. 4 shows the relation between the tensile stress and the elongation of M type specimens as an example. Tensile stress  $\sigma_o$  is obtained by dividing tensile load  $P$  by the minimum sectional area including the pin hole as shown by the following equation<sup>(2),(5)</sup>:

$$\sigma_o = \frac{P}{2(R-r)t} \dots\dots\dots(1)$$

As is clearly seen from Fig. 4, the relation between the tensile stress and elongation of the specimen is similar to the tensile strength curve of mild steel used as the specimen material. The tensile stress  $\sigma_{oy}$ , where the elongation of specimens is deviated from the linear relation, differs according to each joint profile as shown in Table 2, and it decreases as outer radius ratio  $R/r$  increases. Since tensile stress differences according to the plate thickness of specimens is small in all joint profiles, these values are obtained as an average value in each joint profile. Tensile stress  $\sigma_{oy}$  is called joint yield strength in this paper.

#### 3.2 Stress concentration factor

Fig. 5 shows an example of the relation between the tensile stress and strain at each part of the M-type specimen. The strain of gauges ② and ③ on the side face of the pin hole shows that the tensile stress is largely concentrated at this part because the gradient of the curve

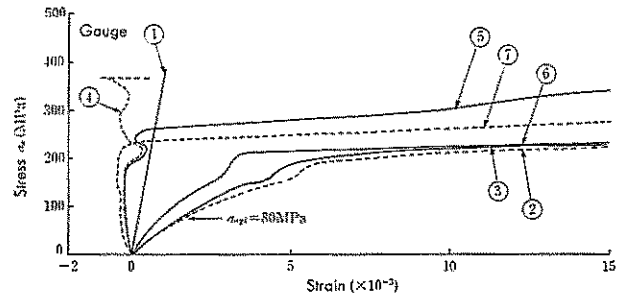


Fig. 5 Relation between tensile stress and strain (M-2)

is the least on the tensile side. Tensile stress  $\sigma_{oyi}$ , where the gauges ② and ③ reach the yield stress of the specimen material, are listed in Table 2 for each joint profile. In this paper,  $\sigma_{oyi}$  is called the local yield stress of joints. The relation between elastic stress concentration factor  $\alpha$  on the side face of the pin hole by  $\sigma_o$  in equation (1) and outer radius ratio  $R/r$  is linear within the experimental range of this study as shown in Fig. 6.

$$\alpha = 0.8 + 1.3 (R/r) \dots\dots\dots(2)$$

The experimental value is larger than the value in reference (2) shown in Fig. 6. This is assumed to have been caused by the clearance between the pin hole and the pin.

The tensile stress of the pin tip at gauge ⑥ locally starts yielding slower when compared with the side face of the pin hole at gauges ② and ③. The strain of gauges ②, ③, ⑥ and ⑦ abruptly increases on the tension side when the stress exceeds joint yield strength  $\sigma_{oy}$ .

#### 3.3 Tensile strength and fracture mode

Fig. 7 shows typical examples of the fracture modes or the final deformation mode of each joint in the tensile test. The S-type specimen shows a cup and corn type rupture on the face perpendicular to the tensile load on the side face of the pin hole. In this case, the center of the rupture plane is fibrous, and the shearing rupture appears outside the joint. For the M-type specimen, ruptures are produced along the shearing deformation

Table 2 Arrangement of tensile test result

Specimen	Local Yield Strength (MPa)		Yield Strength as Joint (MPa)		Tensile Strength (MPa)		Stress Concentration factor $\alpha$	$\frac{\sigma_{oy}}{\sigma_{oyi}}$	$\frac{\sigma_{oy}}{\sigma_{ob}}$
	$\sigma_{oyi}$	$\tau_{oyi}$	$\sigma_{oy}$	$\tau_{oy}$	$\sigma_{ob}$	$\tau_{ob}$			
S	95	42	225	101	410	183	2.8	2.4	0.55
M	80	46	180	104	370	213	3.4	2.3	0.49
L	66	43	155	102	340	223	4.1	2.3	0.46

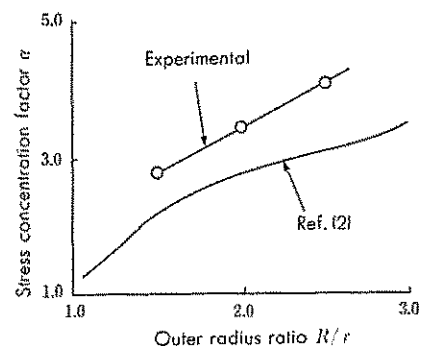


Fig. 6 Relation between stress concentration factor and outer radius ratio

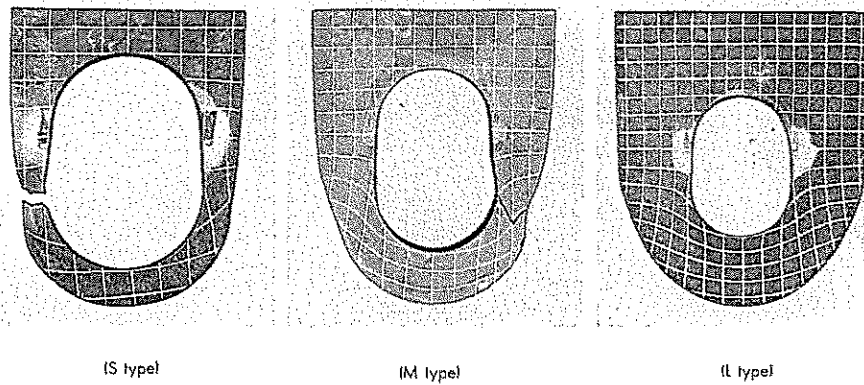


Fig. 7 Fracture mode of each joint profile

to the outside of the joint. For the L-type specimen, no rupture is seen due to limitations of the testing machine. However, remarkably, the shear deformation appears in the tensile load direction area from the side face of the pin hole to the joint tip.

The tensile strength at each joint profile is shown in Table 2 as  $\sigma_{ob}$ . Tensile strength  $\sigma_{ob}$  of the S-type joint is close to the tensile strength of specimen material.  $\sigma_{ob}$  decreases as the outer radius ratio  $R/r$  increases. It is assumed that shearing deformation (tear-out mode<sup>(4)</sup>), since the pin tends to tear the joint in the tensile load direction, becomes dominant for large  $R/r$  specimens.

### 3.4 Analysis by the finite element method

By using the elastic-plastic finite element method, the relation between the tensile stress and the deformation was examined. The work hardening condition is set from results of the tensile test of the specimen material. General-purpose finite element program MARC<sup>(6)</sup> is used under the conditions of Mises yield criterion, the isotropic hardening rule, and the incremental theory of plasticity. Eight-node plane stress elements and gap elements, which simulate the clearance between pins and pin holes, are employed. Fig. 8 compares calculated values and experimental values for changes of strain at each part as well as the displacement about the M-type specimen as an example. As can be seen, calculated values and experimental values coincide.

Fig. 9 shows the expansion pattern of the yield region, for M-type specimen as an example obtained from the calculation over a range up to where the tensile stress exceeds the yield strength of joints. The region shown as a yield region introduces contours of a very small equivalent plastic strain ( $5 \times 10^{-4}$ ) from the calculation points in the elements. As the tensile stress increases, the local yield expands from point A (in Fig. 9) on the side face of the pin hole. From a certain tensile stress, the yield begins from the joint tip at point D and expands.

The yield regions from point A and D are coupled with each other in the region on the line from points A to C. The deformation of the joint abruptly increases

after those two yield regions connect. The tensile stress in this stage is almost equal to yield stress as joint  $\sigma_{oy}$  obtained by the experiment.

### 3.5 Design examination

Table 2 lists the results obtained from this experiment, indicating the pattern of strength values by the tensile stress  $\sigma_o$  using equation (1) and those by the shearing stress  $\tau_o$  defined by the following equation:

$$\tau_o = \frac{P}{2\sqrt{R^2 - r^2} t} \dots\dots\dots(3)$$

Its denominator shows the sectional area where the pin tends to tear-out the joint (sectional area of 2AC in Fig. 2).

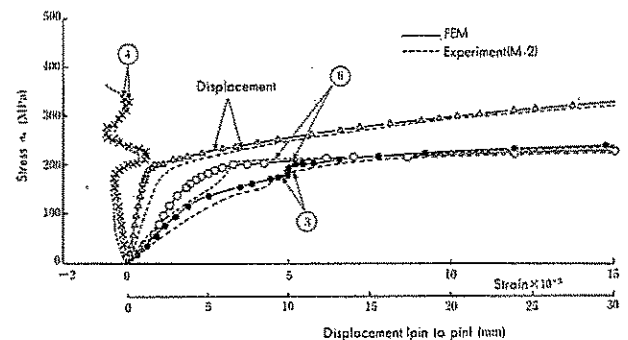


Fig. 8 Comparison of FEM and experimental result (M type)

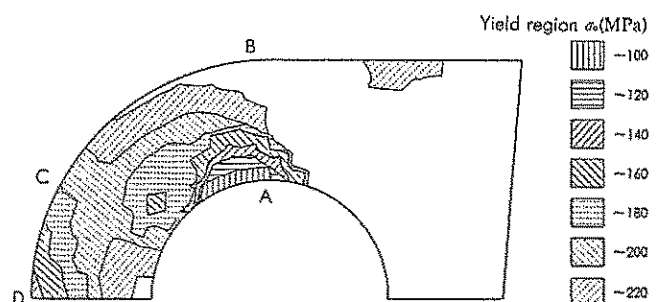


Fig. 9 Expansion of yield region (FEM) (M type)

From these experimental results, yield stress strength  $\sigma_{oy}$  can be represented by the following equation (4) using tensile stress  $\sigma_o$  as the reference and by  $\alpha$  in equation (2), because the  $\sigma_{oy}$  to  $\sigma_{oyi}$  ratio is almost kept constant as 2.3 for all joint profiles.

$$\sigma_{oy} = \frac{2.3 \sigma_y}{0.8 + 1.3 (R/r)} \dots\dots\dots(4)$$

Where,  $\sigma_y$  is the yield stress of the joint material. Also, joint yield strength  $\tau_{oy}$  can be presented by the following experimental equation (5) when shearing stress  $\tau_o$  is used as the reference, because the yield strength at the joint is kept almost constant, irrespective of joint profiles.

$$\tau_{oy} = 0.38 \sigma_y \dots\dots\dots(5)$$

Equation (5) is simple and indicates the shearing strength which may be related to the yield strength of joints. Conversely, equation (4) contains the stress concentration factor of the maximum stress concentration part: It is practically developmental, because the fatigue strength should be evaluated in crane structures<sup>(7)</sup>.

Tensile strength of joints is not kept constant by the arrangement of either tensile stress  $\sigma_o$  or shearing stress  $\tau_o$  due to a difference of the fracture mode according to joint profiles as described above. It may generally be said that for crane structures using mild steel materials, the safety evaluation can practically be done by using the yield strength as joint and the safety factor in the rule<sup>(7)</sup>, because the yield ratio  $\sigma_{oy}/\sigma_{ob}$  of all joint profiles is smaller than the yield ratio of specimen materials.

#### 4. Conclusion

The following useful design information about the strength of the pin joints for crane structures has been obtained.

- (1) The yield strength for a joint can be obtained by equation (4), when the tensile stress in the minimum sectional area containing the pin hole is used as the reference.  
AISC specifies the allowable stress by using this tensile stress as the reference, but it does not take the effect of the outer radius ratio  $R/r$  into consideration.
- (2) The yield strength for a joint can also be obtained by equation (5) irrespective of the outer radius ratio  $R/r$ , when the shearing stress for the tear-out mode is employed as the reference.
- (3) According to analysis by the finite element method, the yield of a joint is produced by the tensile load which connects the yield region from the side face of the pin hole to the yield region from the joint tip.
- (4) The fracture mode of joints differs according to the outer radius ratio  $R/r$ .

#### REFERENCES

- (1) H. Reissner and F. Strauch: Ingenieur-Arch., Vol. 4 1933 481
- (2) M. Nishida: Stress Concentration, 1967 699., Morikita Publication
- (3) Korkut M.D.: Machine Design 9-28 1961 163
- (4) A. Blake: Design News 6-17 1974 76
- (5) AISC: Specification for the Design, Fabrication and Erection of Structural Steel for Buildings 1978 5-18
- (6) Marc Analysis Research Corporation, User Information Manual Volume A 1984 6
- (7) JISB8821: Specification for the Design of Crane Structures 1976 6